

Tools for High-dimensional Bell Basis Distinguishability with LELM Devices

Thomas Schneider

Theresa Lynn, Advisor

Second Reader, Reader



Department of Physics

May, 2019

Copyright © 2019 Thomas Schneider.

The author grants Harvey Mudd College and the Claremont Colleges Library the nonexclusive right to make this work available for noncommercial, educational purposes, provided that this copyright statement appears on the reproduced materials and notice is given that the copying is by permission of the author. To disseminate otherwise or to republish requires written permission from the author.

Abstract

For many quantum information protocols, it is useful to be able to reliably differentiate between several entangled states. Practical restrictions on building quantum devices have pushed theorists towards studying the power of quantum devices limited to locally manipulating their particles. In this thesis, we are concerned with determining the power of linear evolution, local measurement (LELM) devices for distinguishing sets of Bell states. The qubit case has been fully studied previously: projective LELM devices cannot distinguish all four qubit Bell states, they can only reliably distinguish three. The question of how many qudit Bell states a projective LELM device can reliably distinguish is still open. In this thesis, we explore various computational and mathematical tools for investigating this question.

Contents

Abstract	iii
Acknowledgments	xi
1 Introduction	1
2 Background	3
2.1 Quantum Information and Entanglement	3
2.2 Linear Evolution Local Measurement Apparatuses	5
2.3 The Distinguishability Problem	6
3 Previous Work	7
3.1 Work on Equivalent Inputs	7
3.2 Work on Hyperentanglement	7
4 Characterizing Equivalent Inputs	9
4.1 A Group of Transformations	9
4.2 The $d = 4$ Case	17
5 Comparing the $d = 4$ Bell Basis with the Hyperentangled Basis	21
5.1 Which Reductions are Possible?	21
5.2 An Experimental Approach	21
Bibliography	23

List of Figures

2.1	A LELM apparatus.	6
4.1	An LELM device, with the focus of this chapter highlighted in green.	10
4.2	Some basic actions on $S = \{ \Psi_0^0\rangle, \Psi_0^1\rangle, \Psi_0^2\rangle, \Psi_1^2\rangle\}$	11
4.3	A table of the first 25 values for the size of the stabilizer of $\{ \Psi_0^0\rangle\}$ and the size of G_d	18
4.4	A table giving the number of elements for each stabilizer size.	19

List of Tables

Acknowledgments

I would like to thank Professor Theresa Lynn for doing all of the things I could have possibly wanted an advisor to do, and doing those things very well. I would also like to thank Anna Barth, with whom I developed almost as many ideas as we shot down. And more generally, I would like to thank the people at Harvey Mudd College—it is them that have made this experience worth it.

Chapter 1

Introduction

The central question of this thesis—How many qudit Bell states can a projective LELM device reliably distinguish?—is of both practical and theoretical importance.

Measurements in the Bell basis are necessary for many quantum information protocols, such as quantum teleportation and superdense coding. In fact, being able to reliably distinguish sets of maximally entangled vectors (of which Bell bases are canonical examples)

(8)

In Chapter 2 provides background for understanding the problem of LELM distinguishability. This includes information about the basics of quantum information, entanglement,

Chapter 3 outlines relevant progress made towards

In particular, it focuses on 1) group for $d=3$ and 2) hyperentangled case.

Chapter 4 presents the major results, providing a generalization of the group of transformations discussed in Chapter 3.¹

In Chapter 5, we discuss attempts to utilize information about the hyperentangled Bell basis

¹In particular, we generalize the group to higher d s.

Chapter 2

Background

2.1 Quantum Information and Entanglement

This section will focus on the basics of quantum information that are relevant to understanding the Bell basis distinguishability question for LELM devices.

2.1.1 Bits, Qubits, Qutrits, Qudits

The basic unit of classical information is the bit, which can take on either the value 0 or 1. A bit is exactly enough information necessary to describe the state of a two-state system. A common example is that of a light-switch, for which 0 could represent “off” and 1 could represent “on.”

The quantum analog of the bit is the *qubit*. Qubits also describe two-state systems; however, they allow for specific combinations of possibilities. Qubits can take on either the value $|0\rangle$, $|1\rangle$, or any value of the form

$$|b\rangle = \alpha|0\rangle + \beta|1\rangle$$

where α and β are complex numbers normalized such that $|\alpha|^2 + |\beta|^2 = 1$. The notation $|\rangle$ is called a *ket*. Another way to represent the same qubit is as a column vector

$$b = \begin{pmatrix} \alpha \\ \beta \end{pmatrix}$$

but the ket notation is often more efficient.

When one wishes to collect a value from a qubit, they *measure* it. Then the qubit ‘collapses’ and unambiguously become either $|0\rangle$ or $|1\rangle$. The probability of the qubit collapsing to each state are determined by α and β ,

4 Background

with probability $|\alpha|^2$ of collapsing to $|0\rangle$ and probability $|\beta|^2$ of collapsing to $|1\rangle$.

The set of all possible values for a qubit is a vector space of dimension two. One basis for this space is $\{|0\rangle, |1\rangle\}$. Measurements can be performed in any orthogonal basis. Other common orthogonal bases include

$$\left\{ \frac{1}{\sqrt{2}}|0\rangle + \frac{1}{\sqrt{2}}|1\rangle, \frac{1}{\sqrt{2}}|0\rangle - \frac{1}{\sqrt{2}}|1\rangle \right\}$$

and

$$\left\{ \frac{1}{\sqrt{2}}|0\rangle + \frac{i}{\sqrt{2}}|1\rangle, \frac{1}{\sqrt{2}}|0\rangle - \frac{i}{\sqrt{2}}|1\rangle \right\}.$$

If a qubit $|b\rangle$ is measured in the orthogonal basis $\{|x\rangle, |y\rangle\}$, then there is a $|\langle b|x\rangle|^2$ probability of measuring $|x\rangle$ and a $|\langle b|y\rangle|^2$ probability of measuring $|y\rangle$. Here, we've used the notation $\langle b|x\rangle$ to represent the inner product of $|b\rangle$ and $|x\rangle$. Moreover, the symbol $\langle|$ is called a *bra*, and it is used to represent the conjugate transpose of a ket. Hence, the conjugate transpose of the 'column' vector $\frac{1}{\sqrt{2}}|0\rangle - \frac{i}{\sqrt{2}}|1\rangle$ would be the 'row' vector $\frac{1}{\sqrt{2}}\langle 0| + \frac{i}{\sqrt{2}}\langle 1|$.

Sometimes—such as in this thesis—we have the desire to represent systems that can take on more than two states. *Qutrits* represent systems that can take on three values, and *qudits* refer to the generalizations of qubits that represent systems with an arbitrary (but finite) number of states. We write an arbitrary qutrit as

$$|t\rangle = \alpha|0\rangle + \beta|1\rangle + \gamma|2\rangle$$

and an arbitrary qudit as

$$|q\rangle = \alpha_0|0\rangle + \alpha_1|1\rangle + \cdots + \alpha_{d-1}|d-1\rangle.$$

The numerical labels inside the kets can of course be changed without affecting any of the physics or the math.

Another useful generalization to consider is that of multi-particle systems. In classical computing, two-bit systems can take on four values: 00, 01, 10, and 11. In the notation of quantum information, we write these four values as:

$$|0\rangle \otimes |0\rangle, |0\rangle \otimes |1\rangle, |1\rangle \otimes |0\rangle, \text{ and } |1\rangle \otimes |1\rangle.$$

The \otimes symbol is used because our $|0\rangle$ and $|1\rangle$ kets are vectors, and their product is an element of a tensor product space. Similarly to how a qubit can be an arbitrary normalized linear combination of $|0\rangle$ and $|1\rangle$, states in

a multi-particle system can be any normalized linear combination of the vectors $|0\rangle \otimes |0\rangle$, $|0\rangle \otimes |1\rangle$, $|1\rangle \otimes |0\rangle$, and $|1\rangle \otimes |1\rangle$. Often we will omit the \otimes and write $|0\rangle \otimes |0\rangle$ as either $|0\rangle|0\rangle$ or as $|00\rangle$.

2.1.2 Entanglement

Entanglement refers to any multi-particle quantum state that cannot be represented as

Two examples of non-entangled quantum states are $|11\rangle$ and $\frac{1}{\sqrt{2}}|11\rangle$

A state is maximally entangled if knowing information about one

2.1.3 The Basics of Bell Bases

The canonical Bell basis consists of the four states:

$$|\Phi^+\rangle = \frac{1}{\sqrt{2}} (|0\rangle|0\rangle + |0\rangle|0\rangle)$$

$$|\Phi^-\rangle = \frac{1}{\sqrt{2}} (|0\rangle|0\rangle - |0\rangle|0\rangle)$$

$$|\Psi^+\rangle = \frac{1}{\sqrt{2}} (|0\rangle|1\rangle + |1\rangle|0\rangle)$$

$$|\Psi^-\rangle = \frac{1}{\sqrt{2}} (|0\rangle|1\rangle - |1\rangle|0\rangle)$$

The Bell basis is a basis of entangled states for a two-particle system. If each particle has dimension d , then the Bell basis is:

$$\left\{ |\Psi_c^p\rangle = \frac{1}{\sqrt{d}} \sum_{j=0}^{d-1} \omega^{pj} |j\rangle |j+c \pmod{d}\rangle \text{ such that } c, p \in \mathbb{Z} \text{ and } 0 \leq c, p < d \right\}$$

where $\omega = e^{i2\pi/d}$ is a primitive d th root of unity. Thus, for two d -dimensional particles, there are d^2 states in the Bell basis.

2.2 Linear Evolution Local Measurement Apparatuses

A Linear Evolution Local Measurement (LELM) apparatus (Figure 2.1) has two main parts to it. The Linear Evolution part of the LELM apparatus refers to how the device can linearly evolve either particle separately, but cannot

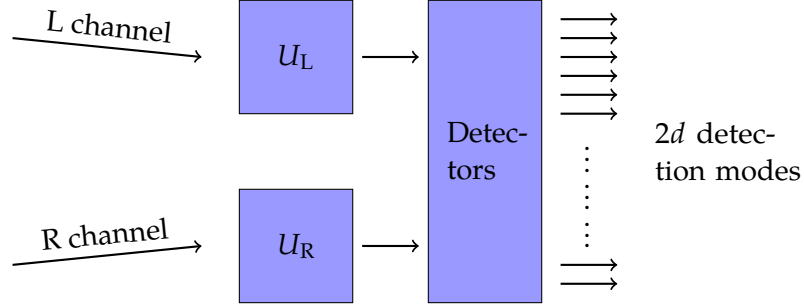


Figure 2.1 A LELM apparatus.

manipulate a particle based on the value of the other. So, for example, LELM devices cannot perform a controlled bit-shift. The Local Measurement part of the LELM apparatus refers to how measurements are restricted to acting on a single particle at a time. Thus, a LELM apparatus takes in two particles, and outputs two detection events or ‘clicks’.

The basis of single-particle states is:

$$\mathcal{B}_{\text{single-particle}} = \{|0, L\rangle, |0, R\rangle, |1, L\rangle, |1, R\rangle, \dots, |d-1, L\rangle, |d-1, R\rangle\}$$

The basis is of size $2d$, since each particle can either be from the left channel or the right channel.

A pair of two detector modes is called a detection signature. Each detection mode is an element in the span of $\mathcal{B}_{\text{single-particle}}$. However, if $|i\rangle$ and $|j\rangle$ are detection modes then when determining their combined detection signature, we cannot simply take $|i\rangle \otimes |j\rangle$, since that may include inputs where two particles are coming from the same channel. Thus, we introduce the P_{LR} projection operator, which removes all elements of $\mathcal{B}_{\text{single-particle}} \times \mathcal{B}_{\text{single-particle}}$ of the form $|*, L\rangle|*, L\rangle$ or $|*, R\rangle|*, R\rangle$ and renormalizes resulting the state.

2.3 The Distinguishability Problem

2.3.1 Motivation

-practical (cite) -mathematical (cite)

2.3.2 Formalization

Chapter 3

Previous Work

3.1 Work on Equivalent Inputs

3.1.1 Leslie's Work

3.1.2 Other Work

3.2 Work on Hyperentanglement

Chapter 4

Characterizing Equivalent Inputs

When considering an LELM device, it's convenient to break the device into two components: the linear evolution section, which is comprised of the L and R channels as well as the transformations U_L and U_R , and the local measurement section, which is comprised of the $2d$ detection modes. In this chapter, we are completely concerned with inputs into our LELM device and what can be done on them by local operations. We focus on the question of which subsets of a Bell basis can be transformed into one another using only local operations (if so, we call these sets *equivalent*).

This question of determining equivalence classes of input sets is interesting in its own right, but is also useful for proving indistinguishability results. Once we prove that some subset of Bell states cannot be distinguished by an LELM device, we've shown that no equivalent subset can be distinguished by an LELM device. Generally, we hope to find that the equivalence classes are as large as possible since then results about particular sets of Bell states carry the most weight.

4.1 A Group of Transformations

One approach to answering the question "What subsets of the Bell bases can be transformed into each other by local operations?" is to look at transformations of the form $U_L \otimes U_R$ that permute the Bell basis. In his senior thesis, Nathaniel Leslie presents a set of four transformations for the $d = 3$ case that permute the Bell basis. Each transformation has a

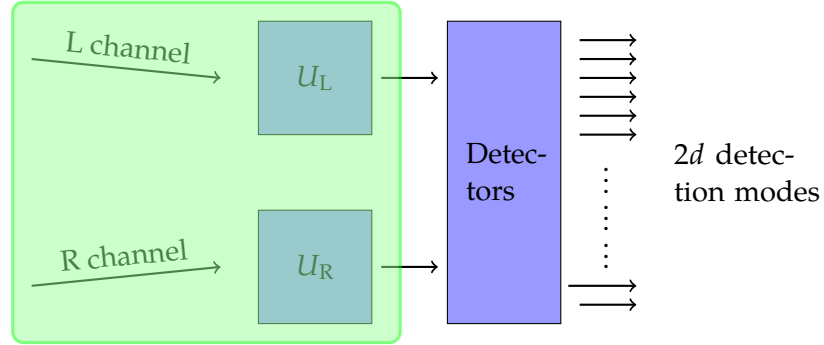


Figure 4.1 An LELM device, with the focus of this chapter highlighted in green.

simple corresponding description in terms of tic-tac-toe diagrams. The four rotations that Nathaniel looked at were:

\hat{i}_p : Cycle all the columns right.

\hat{i}_c : Cycle all the rows down.

\hat{s}_p : Shift the rows in a staggered manner. Leave the first ($c = 0$) row unchanged. Move the second ($c = 1$) row one to the right. Move the third ($c = 2$) row two to the right. [Note: moving a row two the right is the same as moving it one to the left.]

\hat{s}_c : Move the columns in a staggered manner. Leave the first ($p = 0$) column unchanged. Move the second ($p = 1$) column one down. Move the third ($p = 2$) column two down.

We've chosen to name these four translations \hat{i}_p , \hat{i}_c , \hat{s}_p , \hat{s}_c for increment phase, increment correlation class, stagger phase, stagger correlation class. The way we have defined these transformations is in terms of our diagram, so we need to describe them in terms of separate operations on left and right channel particles, which we will do shortly. But first, it's useful to see how the group generated by these simple transformations acts on subsets of the Bell basis. Let $G_d = \langle i_p, i_c, s_p, s_c \rangle$ and let $S = \{|\Psi_0^0\rangle, |\Psi_0^1\rangle, |\Psi_0^2\rangle, |\Psi_1^2\rangle\}$, the subset from Figure 4.2, which also depicts the same set S after the operations \hat{i}_p , \hat{i}_c , \hat{s}_p , and \hat{s}_c .

Another way we can describe these transformations is by what they send a generic state to:

$$\hat{i}_p: |\Psi_c^p\rangle \rightarrow |\Psi_c^{p+1}\rangle$$

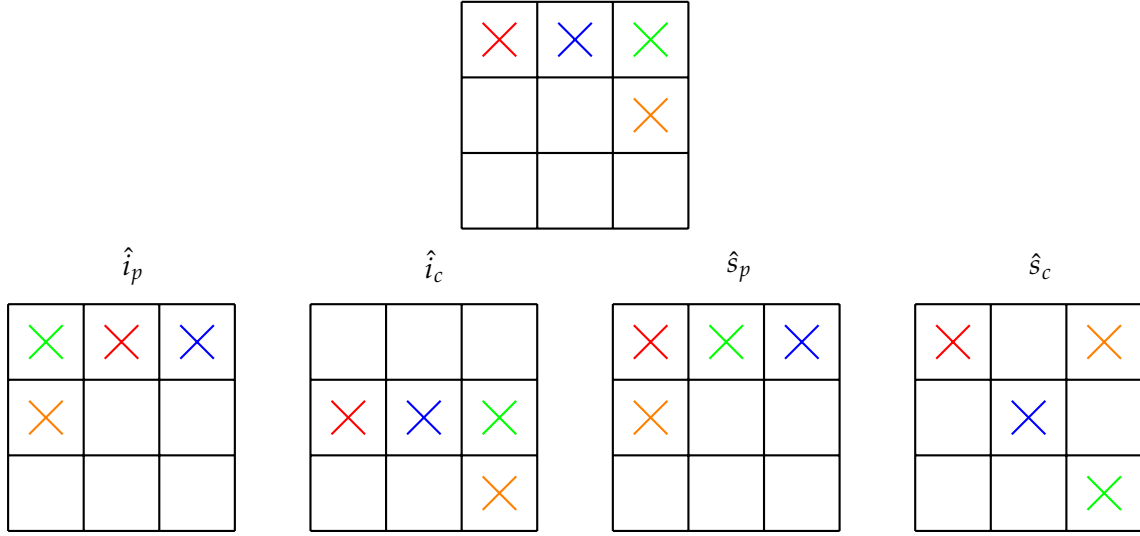


Figure 4.2 Some basic actions on $S = \{|\Psi_0^0\rangle, |\Psi_0^1\rangle, |\Psi_0^2\rangle, |\Psi_1^2\rangle\}$

$$\hat{i}_c: |\Psi_c^p\rangle \rightarrow |\Psi_{c+1}^p\rangle$$

$$\hat{s}_p: |\Psi_c^p\rangle \rightarrow |\Psi_c^{p+c}\rangle$$

$$\hat{s}_c: |\Psi_c^p\rangle \rightarrow |\Psi_{c+p}^p\rangle$$

4.1.1 Defining the Transformations

Now it's time for us to define the transformations \hat{i}_p , \hat{i}_c , \hat{s}_p , and \hat{s}_c in terms of operations on single-particles. Here, we'll switch to a more condensed notation for denoting which channel a particle came from, using a subscript. As usual, arithmetic is done mod d .

\hat{i}_p : To do this transformation, we cycle the phase in the left channel:

$$\hat{i}_c|k\rangle_L \rightarrow \omega^k|k\rangle_L \quad \text{and} \quad \hat{i}_c|k\rangle_R \rightarrow |k\rangle_R$$

where $\omega = e^{i2\pi/d}$. This increments the phase.

\hat{i}_c : To do this transformation, we cycle the variable in the right channel:

$$\hat{i}_p|k\rangle_L \rightarrow |k\rangle_L \quad \text{and} \quad \hat{i}_p|k\rangle_R \rightarrow |k+1\rangle_R.$$

This increments the correlation class.

\hat{s}_p : This transformation is trickier, so we'll show how to derive it. Instead of simply guessing the solution like for the incrementing transformations, we'll begin by describing symbolically a semi-generic transformation on the left channel particle looks like.¹ The free variables in this our description (i.e. x_0, x_1, \dots, x_{d-1}) represent information about how the phase of each left-particle ket changes. They're defined as such:

$$\begin{aligned}\hat{s}_p|0\rangle_L &\rightarrow \omega_0^x|0\rangle_L \\ \hat{s}_p|1\rangle_L &\rightarrow \omega_1^x|1\rangle_L \\ &\vdots \\ \hat{s}_p|d-1\rangle_L &\rightarrow \omega_{d-1}^x|d-1\rangle_L\end{aligned}\tag{4.1}$$

Next, we'll derive from our desired behavior of \hat{s}_p what the values we need for our x_i 's. Since $\hat{s}_p|\Psi_0^p\rangle = |\Psi_0^{p+0}\rangle = |\Psi_0^p\rangle$, then we must have that $\hat{s}_p|d-1\rangle_R \rightarrow \omega^{-x_{d-1}}|d-1\rangle_R$. This guarantees that $\hat{s}_p|(d-1)(d-1)\rangle \rightarrow \omega^{-x_{d-1}}\omega^{x_{d-1}}|(d-1)(d-1)\rangle = |(d-1)(d-1)\rangle$.

Now, setting $c = 1$ gives us a system of equations. We want \hat{s}_p to increment by 1, up to an overall phase of $\frac{dy}{2\pi}$, meaning:

$$\begin{aligned}\hat{s}_p|\Psi_1^p\rangle &= \hat{s}_p\left(\frac{1}{\sqrt{d}}\left(|0\rangle_L|1\rangle_R + \omega^p|1\rangle_L|2\rangle_R + \omega^{2p}|2\rangle_L|3\rangle_R + \dots + \omega^{(d-1)p}|d-1\rangle_L|0\rangle_R\right)\right) \\ &= \frac{\omega^y}{\sqrt{d}}\left(|0\rangle_L|1\rangle_R + \omega^{p+1}|1\rangle_L|2\rangle_R + \omega^{2p+2}|2\rangle_L|3\rangle_R + \dots + \omega^{(d-1)p+d-1}|d-1\rangle_L|0\rangle_R\right).\end{aligned}\tag{4.2}$$

We have from our definition of \hat{s}_p that:

$$\begin{aligned}\hat{s}_p|\Psi_1^p\rangle &= \hat{s}_p\left(\frac{1}{\sqrt{d}}\left(|0\rangle_L|1\rangle_R + \omega^p|1\rangle_L|2\rangle_R + \dots + \omega^{(d-1)p}|d-1\rangle_L|0\rangle_R\right)\right) \\ &= \frac{1}{\sqrt{d}}\left(\omega^{x_0-x_1}|0\rangle_L|1\rangle_R + \omega^{x_1-x_2+p}|1\rangle_L|2\rangle_R + \dots + \omega^{x_{d-1}-x_0+(d-1)p}|d-1\rangle_L|0\rangle_R\right).\end{aligned}\tag{4.3}$$

¹By semi-generic, we mean that we will restrict ourselves to looking at the subset transformations where the correlation class is fixed but the resulting phases are completely generic.

Matching the exponents of the ω 's, we get the system of equations:

$$\begin{aligned}
 x_0 - x_1 &= y \\
 p + x_1 - x_2 &= y + p + 1 \\
 2p + x_2 - x_3 &= y + 2p + 2 \\
 &\vdots \\
 (d-1)p + x_{d-1} - x_0 &= y + (d-1)p + d - 1,
 \end{aligned} \tag{4.4}$$

which we can re-write such that we can solve it by recursively plugging an equation for x_{k+1} into the equation for x_k . We have,

$$\begin{aligned}
 x_0 &= x_1 + y \\
 x_1 &= x_2 + y + 1 \\
 x_2 &= x_3 + y + 2 \\
 &\vdots \\
 x_{d-1} &= x_0 + y + d - 1.
 \end{aligned} \tag{4.5}$$

This tells us that

$$x_0 = x_0 + dy + \sum_{k=0}^{d-1} k = x_0 + dy + \frac{d(d-1)}{2},$$

which we can solve to get that $y = \frac{1-d}{2} \pmod{d}$. Let's take $y = (d+1)/2$. We can also arbitrarily choose $x_0 = 0$ to get values for x_0, x_1, \dots, x_{d-1} :

$$\begin{aligned}
 x_1 &= x_0 - y - 0 \Rightarrow x_1 = -y \\
 x_2 &= x_1 - y - 1 \Rightarrow x_2 = -2y - 1 \\
 x_3 &= x_2 - y - 2 \Rightarrow x_3 = -3y - 3 \\
 &\vdots \\
 x_{d-1} &= x_0 + y + d - 1 \Rightarrow x_{d-1} = \cancel{-(d-1)y} \overset{y}{\rightarrow} - \sum_{k=0}^{d-1} k = (d+1)/2 - d/2 = 1/2.
 \end{aligned} \tag{4.6}$$

Now we must check that this transformation sends $|\Psi_c^p\rangle$ to $|\Psi_c^{p+c}\rangle$ in

general. We have that:

$$\begin{aligned}
 \hat{s}_p |\Psi_c^p\rangle &= \hat{s}_p \left(\frac{1}{\sqrt{d}} \left(|0\rangle_L |0+c\rangle_R + \omega^p |1\rangle_L |1+c\rangle_R + \cdots + \omega^{(d-1)p} |d-1\rangle_L |d-1+c\rangle_R \right) \right) \\
 &= \frac{\omega^{y_c}}{\sqrt{d}} \left(|0\rangle_L |0+c\rangle_R + \omega^{p+c} |1\rangle_L |1+c\rangle_R + \cdots + \omega^{(d-1)p+(d-1)c} |d-1\rangle_L |d-1+c\rangle_R \right) \\
 &= \frac{1}{\sqrt{d}} (\omega^{x_0-x_c} |0\rangle_L |0+c\rangle_R + \omega^{x_1-x_{c+1}+p} |1\rangle_L |1+c\rangle_R + \cdots \\
 &\quad + \omega^{x_{d-1}-x_{d-1+c}+(d-1)p} |d-1\rangle_L |d-1+c\rangle_R).
 \end{aligned} \tag{4.7}$$

From this, we get the system of equations:

$$\begin{aligned}
 0 + x_0 - x_c &= y_c + 0 + 0 \\
 p + x_1 - x_{c+1} &= y_c + c + p \\
 2p + x_2 - x_{c+2} &= y_c + 2c + 2p \\
 &\vdots \\
 (d-1)p + x_{d-1} - x_{c+d-1} &= y_c + (d-1)c + (d-1)p
 \end{aligned} \tag{4.8}$$

which can be re-arranged to get:

$$\begin{aligned}
 x_0 &= x_c + y_c + 0 \\
 x_1 &= x_{c+1} + y_c + c \\
 x_2 &= x_{c+2} + y_c + 2c \\
 &\vdots \\
 x_{d-1} &= x_{c+d-1} + y_c + (d-1)c
 \end{aligned} \tag{4.9}$$

Now we wish to look back to the $c = 1$ case in the system of equations Equation 4.5. Notice that if we plug in the second equation ($x_1 = x_2 + y + 1$) into the first equation, then plug the third equation into ($x_2 = x_3 + y + 2$), and we repeat this process c times, then we get:

$$x_0 = x_c + cy + 1 + 2 + \cdots + (c-1) = x_c + cy + c(c-1)/2. \tag{4.10}$$

Moreover, we can perform a similar process of cascading plugging-in of equations to get:

$$x_k = x_{k+c} + cy + k + (k+1) + \cdots + (k+c-1) = x_{k+c} + cy + c(c-1)/2 + ck. \tag{4.11}$$

Thus, the system equations Equation 4.5 implies that:

$$\begin{aligned}
 x_0 &= x_c + cy + c(c-1)/2 \\
 x_1 &= x_{c+1} + cy + c(c-1)/2 + c \\
 x_2 &= x_{c+2} + cy + c(c-1)/2 + 2c \\
 &\vdots \\
 x_{d-1} &= x_{d-1+c} + cy + c(c-1)/2 + (d-1)c.
 \end{aligned} \tag{4.12}$$

Comparing this to the system of equations Equation 4.9, we find that setting $y_c = cy + c(c-1)/2$, that Equation 4.5 begin solvable implies that Equation 4.9 is solvable. And we're done— \hat{s}_p actually exists!

\hat{s}_c : Instead of constructing \hat{s}_c directly, we'll first show that we are able to swap the phase and the correlation class. The way we'll do this is by performing the inverse Quantum Fourier Transform to the particle in the left channel and the Quantum Fourier Transform to the particle in the right channel. That is, if $|\Psi_c^p\rangle = \frac{1}{\sqrt{d}} \sum_{j=0}^{d-1} \omega^{pj} |j\rangle |j+c\rangle$, then we perform the transformations:

$$|j\rangle \mapsto \frac{1}{\sqrt{d}} \sum_{k=0}^{d-1} \omega^{-kj} |k\rangle \quad \text{and} \quad |j+c\rangle \mapsto \frac{1}{\sqrt{d}} \sum_{l=0}^{d-1} \omega^{l(j+c)} |l\rangle. \tag{4.13}$$

Thus,

$$\begin{aligned}
 |\Psi_c^p\rangle &= \frac{1}{\sqrt{d}} \sum_{j=0}^{d-1} \omega^{pj} |j\rangle |j+c\rangle \mapsto \\
 &= \left(\frac{1}{\sqrt{d}} \right)^3 \sum_{j=0}^{d-1} \omega^{pj} \left(\sum_{k=0}^{d-1} \omega^{-kj} |k\rangle \right) \left(\sum_{l=0}^{d-1} \omega^{l(j+c)} |l\rangle \right) \\
 &= \left(\frac{1}{\sqrt{d}} \right)^3 \sum_{j=0}^{d-1} \sum_{k=0}^{d-1} \sum_{l=0}^{d-1} (\omega^{l-k+p})^j \omega^{lc} |k\rangle |l\rangle \\
 &= \left(\frac{1}{\sqrt{d}} \right)^3 \sum_{k=0}^{d-1} \sum_{l=0}^{d-1} \left[(\omega^{lc} |k\rangle |l\rangle) \left(\sum_{j=0}^{d-1} (\omega^{l-k+p})^j \right) \right]
 \end{aligned} \tag{4.14}$$

The sum $\sum_{j=0}^{d-1} (\omega^{l-k+p})^j$ is d if $l-k+p$ is a multiple of d and the sum is 0 otherwise. Since $0 \leq l, k, p \leq d-1$, we know that $-d+1 \leq$

$l - k + p < 2d - 2$. Thus, if $l - k + p$ is a multiple of d then either $l - k + p = 0$ or $l - k + p = d$. Another way to phrase this, is that the $|k\rangle|l\rangle$ pairs of kets that are kept are exactly the ones that differ by p , where $l - k \equiv p \pmod{d}$. Thus, we have:

$$\begin{aligned}
|\Psi_c^p\rangle &= \frac{1}{\sqrt{d}} \sum_{j=0}^{d-1} \omega^{pj} |j\rangle |j+c\rangle \mapsto \\
&= \left(\frac{1}{\sqrt{d}}\right)^3 \sum_{k=0}^{d-1} \sum_{l=0}^{d-1} \omega^{lc} |k\rangle |k+p\rangle d \\
&= \left(\frac{1}{\sqrt{d}}\right) \sum_{k=0}^{d-1} \omega^{(k+p)c} |k\rangle |k+p\rangle \\
&= \left(\frac{\omega^{kc}}{\sqrt{d}}\right) \sum_{k=0}^{d-1} \omega^{kc} |k\rangle |k+p\rangle = \omega^{kc} |\Psi_p^c\rangle
\end{aligned} \tag{4.15}$$

[Note that $\omega^{(k+p)c} = \omega^{(k+p+d)c}$.]

Thus, we can construct the operation $\hat{s}_c : |\Psi_c^p\rangle \mapsto |\Psi_{c+p}^p\rangle$ by applying the swapping operation, applying \hat{s}_p , then applying and the swapping operation again:

$$\hat{s}_c : |\Psi_c^p\rangle \mapsto |\Psi_p^c\rangle \mapsto |\Psi_p^{c+p}\rangle \mapsto |\Psi_{c+p}^p\rangle. \tag{4.16}$$

Phew, that was quite some algebra. A quick recap what we have done in this section:

- We've looked at the transformations defined in Nathaniel Leslie's thesis (which we've renamed). They are valid only for the $d = 3$ case.
- We've extended the definitions of $\hat{i}_c, \hat{i}_p, \hat{s}_c, \hat{s}_p$ for the general qudit case.
- We've proved that each of the transformations $\hat{i}_c, \hat{i}_p, \hat{s}_c, \hat{s}_p$ take the form of $U_L \otimes U_R$ and are thus implementable in an LELM device.

4.1.2 Orbit-Stabilizer on our Group of Transformations

Let G_d be the group comprised of arbitrary compositions of the transformations $\hat{i}_c, \hat{i}_p, \hat{s}_c, \hat{s}_p$.

We've constructed G in a for a general d . The goal of creating this group is to determine which subsets of Bell states are equivalent, but it's not

necessarily true that the G_d completely characterizes all equivalent inputs. We do, however, have the know the following.

Theorem 1. *If S_1 and S_2 are subsets of the Bell basis, and $gS_1 = S_2$ for some $g \in G$, then S_1 and S_2 are either both distinguishable or both indistinguishable.*

The set of all S such that $gS = S_1$ for some $g \in G$ is called the orbit of S_1 . Letting $\mathcal{S} = \mathcal{P}(S)$ be the set of all subsets of the Bell basis, and $\mathcal{S}_k = \{S \in \mathcal{S} \text{ such that } |S| = k\}$. Our goal is to partition \mathcal{S} into distinct orbits, so that we only need to determine the distinguishability of one element from each orbit. To do this, we'll use the Orbit-Stabilizer Theorem, which tells us that $|G_d| = |\text{Orb}(S)| |\text{Stab}(S)|$ for any $S \in \mathcal{S}$. In general, once we've described G_d , it's much easier to count the size of the stabilizer of an element than the size of its orbit. In order to find $|G_d|$, we can calculate the size of the orbit and the size of the stabilizer for any element. Choosing $S_0 = \{|\Psi_0^0\rangle\}$ allows us to quickly see which elements of G_d are in $\text{Stab}(S_0)$. They are elements of G that can be written only using the two staggering operations (\hat{s}_p and \hat{s}_c). We must now count them. We've done this computationally via an exhaustive search algorithm, the results of which are tabulated in Figure 4.3 (see the appendix for more details). Looking carefully at this table, we can formulate two conjectures:

Conjecture 2. *If $d = p^n$ where p is prime, then the size of G_d is $d^2(p^{3n} - p^{3n-2})$.*

Conjecture 3. *If $d = mn$ where m and n are relatively prime, then $|G_d| = |G_{mn}| = |G_m| |G_n|$.*

These conjectures hold true for $d = 1$ through $d = 25$.

4.2 The $d = 4$ Case

One way to make progress would be to prove the conjectures from the last section. However, it's probably good to check right now to make sure what we're doing is worthwhile—that the equivalence classes are large enough to warrant worrying about them. To do this, we'll decompose G_4 into orbits. We know that for the $d = 4$ case, we can distinguish 4 Bell states whereas every set of Bell states of size 8 is indistinguishable. Let's focus on the case where $d = 4$ and we're looking at sets of Bell states of size $k = 7$. Thus, $|\mathcal{S}_7| = \binom{16}{7} = 11440$.

d	$ \text{Stab}(\{ \Psi_0^0\rangle\}) $	$ G_d $
1	1	1
2	6	24
3	24	216
4	48	768
5	120	3000
6	144	5184
7	336	16464
8	384	24576
9	648	52488
10	720	72000
11	1320	159720
12	1152	165888
13	2184	369096
14	2016	395136
15	2880	648000
16	3072	786432
17	4896	1414944
18	3888	1259712
19	6840	2469240
20	5760	2304000
21	8064	3556224
22	7920	3833280
23	12144	6424176
24	9216	5308416
25	15000	9375000

Figure 4.3 A table of the first 25 values for the size of the stabilizer of $\{|\Psi_0^0\rangle\}$ and the size of G_d

Size of stabilizer	Size of orbit	Number of elements	Number of distinct orbits
1	768	6912	9
2	384	2304	6
3	256	512	2
4	192	1536	8
6	128	128	1
16	48	48	1

Figure 4.4 A table giving the number of elements for each stabilizer size.

For the $d = 4$ case, we can actually just find the orbits explicitly. Calculating the stabilizer for each element of S_7 , we find get the data in the table in Figure 4.4

Overall, we find that there are 27 distinct orbits. Working with 27 elements is still a lot of work, but it's quite a bit better than dealing with 11440 elements.

Chapter 5

Comparing the $d = 4$ Bell Basis with the Hyperentangled Basis

5.1 Which Reductions are Possible?

Find the set of systems of equations that describe the restrictions that define reductions from $d = 4$ Bell basis to the hyperentangled basis.

5.2 An Experimental Approach

5.2.1 Gradient Descent into Madness

Bibliography

- [1] LESLIE, N. Maximal lelm distinguishability of qubit and qutrit bell states using projective and non-projective measurements, 2017.
- [2] PAPADIMITRIOU, C. M. *Computational Complexity*. Pearson, 1993.
- [3] PISENTI, N., GAEBLER, C. P. E., AND LYNN, T. W. Distinguishability of hyperentangled bell state by linear evolution and local projective measurement.
- [4] PISENTI, N. C. Distinguishability of hyper-entangled bell states with linear devices, 2011.
- [5] RIEFFEL, E., AND POLAK, W. *Quantum Computing: A Gentle Introduction*. The MIT Press, 2014.
- [6] SHANG, V. Computational progress towards maximum distinguishability of bell states by linear evolution and local measurement, 2016.
- [7] VAIDMAN, L., AND YORAN, N. Methods for reliable teleportation.
- [8] WERNER, R. F. All teleportation and dense coding schemes.